Available online at www.sciencedirect.com

ScienceDirect

Procedia CIRP 58 (2017) 499 – 504

www.elsevier.com/locate/procedia

16th CIRP Conference on Modelling of Machining Operations

Finite element modeling and validation of chip segmentation in machining of AISI 1045 steel

Ashwin Devotta [a,b]*, Tomas Beno [b], Raveendra Siriki [c], Ronnie Löf [a], Mahdi Eynian [b]

[a] *Sandvik Coromant AB, Mossvägen 10, 81181 Sandviken, Sweden*
[b] *University West, Department of Engineering Science, 46186 Trollhättan, Sweden*
[c] *Sandvik Materials Technology, Storgatan 2, 81181, Sandviken, Sweden*

* Corresponding author. Tel.: +46-70-6163722; fax: +46-262-66180. *E-mail address:* ashwin.devotta@sandvik.com

Abstract

The finite element (FE) method based modeling of chip formation in machining provides the ability to predict output parameters like cutting forces and chip geometry. One of the important characteristics of chip morphology is chip segmentation. Majority of the literature within chip segmentation show cutting speed (v_c) and feed rate (f) as the most influencing input parameters. The role of tool rake angle (α) on chip segmentation is limited and hence, the present study is aimed at understanding it. In addition, stress triaxiality's importance in damage model employed in FE method in capturing the influence of α on chip morphology transformation is also studied. Furthermore, microstructure characterization of chips was carried out using a scanning electron microscope (SEM) to understand the chip formation process for certain cutting conditions. The results show that the tool α influences chip segmentation phenomena and that the incorporation of a stress triaxiality factor in damage models is required to be able to predict the influence of the α. The variation of chip segmentation frequency with f is predicted qualitatively but the accuracy of prediction needs improvement.

Peer-review under responsibility of the scientific committee of The 16th CIRP Conference on Modelling of Machining Operations

Keywords: damage modeling; stress triaxiality; chip segmentation

1. Introduction

Finite element (FE) based machining process models provide the ability to obtain the strain undergone by the workpiece material, the strain rate at which the workpiece material deformed and the heat generated in the primary and secondary deformation zones. With FE, cutting process parameters' influence on the chip morphology can be studied in detail.

Within chip morphology prediction, prediction of transition from continuous to segmented chip is of prime importance as they influence generated temperatures and cutting forces. In addition, segmented chip improves chip breakage and leads to better control of the cutting process. Therefore, chip segmentation modeling is expected to the continuous to segmented chip transition for cutting process parameter variation. Pioneering work in understanding chip segmentation in machining have carried about by Nakayama [1] and Komanduri et al. [2]. Nakayama [1] studied chip segmentation at lower cutting speeds for brittle materials and proposed periodic crack formation as the primary cause. These crack formations were initiated at the free surface edge of the shear plane. Komanduri et al.[2] studied the segmented chip formation at higher cutting speeds for ductile material and proposed the onset of a thermo-plastic instability which originates at the tool edge of the shear plane as the primary cause. Recent work by Wang and Liu [3] combined the theories mentioned above into "mixed mode of ductile fracture and adiabatic shear" theory to predict the continuous to segmented chip transition. They proposed the concept of critical cutting load defined as a multiplication of vc and f. The critical cutting load for AISI 1045 steel was in the range of 0.02 – 0.024 and 0.096 - 0.1 for 7050-T7451 Al alloy while keeping the rake angle (α) a constant of 0°. The chip segmentation boundary took

Peer-review under responsibility of the scientific committee of The 16th CIRP Conference on Modelling of Machining Operations
doi:10.1016/j.procir.2017.03.259

the shape of negative power function with the x-axis defined by vc and y-axis defined by f.

Nomenclature

C_i	temperature coefficients
D	dimensionless cumulative damage
DOC	depth of cut
D_i	Autenrieth damage model coefficient
D_{JCi}	Johnson-Cook damage model coefficient
d_i	Advantedge damage model coefficient
f	feed rate
n	strain hardening coefficient
p	hydrostatic pressure
T	temperature
T_{cut}	cut off temperature
T_0	reference temperature
T_m	melting temperature
T_{tf}	transition temeperature for failure in Autenrieth's damage model
v_c	cutting speed
α	tool rake angle
σ_0	yield stress at reference temperature
σ	yield stress
σ_m	mean stress
$\bar{\sigma}$	equivalent stress
σ	stress tensor
ε^f	strain at failure
$\dot{\varepsilon}_{eq}$	equivalent plastic strain rate
$\dot{\varepsilon}_0$	reference equivalent plastic strain rate
ε^p	plastic strain
$\dot{\varepsilon}$	plastic strain rate
$\dot{\varepsilon}_0^p$	reference plastic strain rate
ε_{cut}^p	cut off plastic strain
ε_i^p	instanteous strain increment
$\varepsilon_{f_i}^p$	instantaneous strain to failure
η	dimensionless hydrostatic pressure parameter

The theories as mentioned above show that chip segmentation is attributed to the shear band formation and is dependent on the workpiece material's response to thermo-mechanical loading in the cutting process. Duan and Wang [4] differentiated from a materials perspective the shear bands formed in machining into transformed shear bands and deformed shear bands. Transformed shear bands are formed in segmented chips during machining of workpiece materials such as hardened alloy steels, titanium alloys, and nickel-base alloys. The transformed shear band formations are attributed to adiabatic heating conditions [5] as proposed byt Komanduri et al [2]. At lower cutting speeds, deformed shear bands are produced in highly strain hardened workpiece materials and are influenced by f and α. This is explained by the crack propagation in the primary deformation zone as proposed by Nakayama [1].

To measure chip segmentation in machining, several parameters are available in literature with chip segmentation frequency being one of the most widely used. In addition, to study the segmented chip morphology, geometrical parameters like maximum chip thickness, minimum chip thickness, and chip segmentation length have been used. Atlati et al.[6] proposed the chip segmentation ratios using the above mentioned geometrical parameters as a global measure of shear strain. In addition, they also proposed the chip segmentation intensity ratio using the equivalent plastic strain inside and outside the shear bands. The equivalent plastic strains are obtained from FE simulations and are a local measure of the strain within the chip. Kouadri et al [7] used the chip segmentation ratios and chip segmentation intensity ratios to study the influence of two different rake angles with varying cutting speeds on chip segmentation in machining of AA202-T351 aluminum alloys. They showed that the v_c has a nonlinear proportionality to chip segmentation and is possible to control the chip morphology by identifying a combination of α and v_c. They also showed that smaller f (0.1 mm/rev) produced continuous chips and larger f (0.3 mm/rev) produced segmented chip for both conditions of α=0° and α=15°.

In FE, chip segmentation is modeled by modifying the material evolution laws. From the background of shear band formation theories described above, one can see that the modification of material evolution laws needs to be based on parameters such as stress triaxiality, Lode angle parameter, (to predict deformed shear bands) and temperature (to predict transformed shear bands). Adiabatic shear banding due to thermal instability leading to transformed shear bands is modeled by incorporating dynamic recrystallization phenomena (TANH model) [8], and modeling of strain at failure as a function of temperature, stress triaxiality, strain rate, lode angle parameter within a damage model could be used to model mixed mode of ductile fracture and adiabatic shear [6,9,10]

Johnson and Cook [10] developed a damage model used widely in metal cutting simulations for the prediction of chip segmentation that models failure at strain (ε^f) as follows

$$\varepsilon^f = \left[D_{JC1} + D_{JC2}e^{-D_{JC3}\eta}\right]\left[1 + D_{Jc4}\, ln\frac{\dot{\varepsilon}_{eq}}{\dot{\varepsilon}_0}\right]\left[1 + D_{JC5}\frac{T-T_0}{T_m-T_0}\right] \quad (1)$$

The equation incorporates stress triaxiality through the dimensionless hydrostatic pressure parameter η and is defined as follows

$$\eta = \frac{\sigma_m}{\bar{\sigma}} = \frac{-\left(\frac{1}{3}\right)tr(\boldsymbol{\sigma})}{\sqrt{\left(\frac{3}{2}\right)\boldsymbol{\sigma}:\boldsymbol{\sigma}}} \quad (2)$$

where σ_m is the first invariant of the stress tensor and $\bar{\sigma}$ is the third invariant of the stress tensor. The inclusion of the stress triaxiality within damage modeling in general was developed by Rice and Tracey [11] in the late 1970s to include the influence of hydrostatic stress on the fracture of ductile materials. The stress triaxiality parameter is used to define the influence of varying loading conditions on material failure. When a material is loaded in a mixed mode of compression, and shear as in machining, stress triaxiality becomes an important parameter to predict material failure accurately. Recent studies by Bai .[12] have shown that in addition to stress triaxiality, lode angle parameter is also an important influencing parameter for three-dimensional loading conditions.

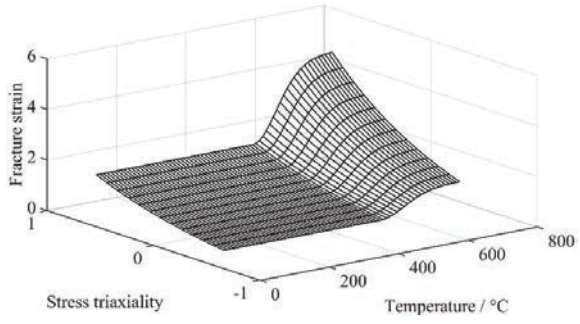

Figure 1 Damage model as a function of temperature and stress triaxiality for AISI 1045 steel according to ref. [13].

Recently, strain at failure in AISI 1045 steel was modeled by, Autenrieth et al.[13]. They showed that strain at failure in AISI 1045 steel (Figure 1) could be modeled as a function of stress triaxiality and temperature as in Eq. (3) where, D_1-D_5, are obtained from Split Hopkinson pressure bar tests and T_{tf} is the transition temperature for failure:

$$\varepsilon^f = \begin{cases} D_1 . e^{\left(-D_2 \frac{p}{\sigma}\right)} & if\ T \le T_{tf} \\ D_1 . e^{\left(-D_2 \frac{p}{\sigma}\right)} \left[D_3 - [D_3 - 1] \left[\left[1 - \left[\frac{T - T_{tf}}{T_m - T_{tf}} \right]^{D4} \right] \right]^{D5} \right] & if\ T \ge T_{tf} \end{cases} \quad (3)$$

Duan and Zhang [14] employed the JC material model and JC damage model to predict chip segmentation in machining of AISI 1045 steel. They showed that with α in the range of -10° to 10° segmented chips are produced when other parameters were kept constant at a v_c of 433 m/min. They also showed that increase in α leads to a reduction in cutting forces with an increase in chip segmentation frequency. The results obtained showed segmented chips for α of -10° and 0° and continuous chip for 10°. In addition to the JC damage model, they also included the modified Zorev friction model which was a function of α.

Most of the reported work have focused on the transition from continuous chip to segmented chip for increasing v_c. Some of the works that have included the influence of α were validated at very high cutting speeds above 400 m/min for AISI 1045 steel. From an industrial perspective, v_c increase leads to increased cutting tool wear and it would be beneficial to obtain segmented chip morphology which improves chip breakage by varying the tool α at a constant v_c [5].

The focus of this work is to assess the influence of stress triaxiality factor in damage model to predict the effect of α on chip segmentation. In addition, it should also be able to predict the transition of chip morphology from continuous to segmented when rake angles and feed rates are varied. The deformation in various parts of the chip is analyzed using electron microscopy and is used to validate the temperature and strain predicted by the FE model.

2. Experimental methods

Orthogonal turning tests are carried out on AISI 1045 steel bar with a diameter of 150 mm, and chips are obtained by varying cutting conditions. No cutting fluids were used. Cutting was carried out on a depth of cut (DOC) of 3 mm on the workpiece face to minimize the influence of grain size variation. The cutting parameters employed in the study are provided in Table 1. The cutting tool material is H13A grade carbide with a TiCN coating. The cutting parameters, f and α are varied as shown in Table 1.

Table 1Cutting parameters used in experimental investigation

v_c (m/min)	150
f (mm/rev)	0.05, 0.10, 0.15, 0.25, 0.40, 0.60
α (°)	-5,0, 5, 10, 15, 20

2.1. Electron microscopy

The chips obtained from the experimental investigation for cutting conditions of f 0.05 mm / rev and rake angles of -5° and 20° are studied in SEM to investigate the deformation pattern in the primary shear zone and the secondary shear zone.

3. FE simulation

The FE simulations were carried out using Thirdwave Advantedge (version 7.2) software specifically developed for the modeling of chip formation in machining [15]. Thirdwave Advantedge is a dynamic explicit Lagrangian formulation based code capable of performing coupled thermo-mechanical transient analysis with adaptive meshing and continuous remeshing capability. In this work, a 2D simulation is carried out where the tool is modeled as a rigid-perfectly elastic body. The tool geometry is modeled using the software's inbuilt capability owing to the simple tool geometry employed in this work. A schematic representation of the workpiece and tool with the relevant cutting parameters is shown in Figure 2.

In addition to the predefined material database available in the software, workpiece material can also be defined using Power law damage model with temperature-dependent thermal

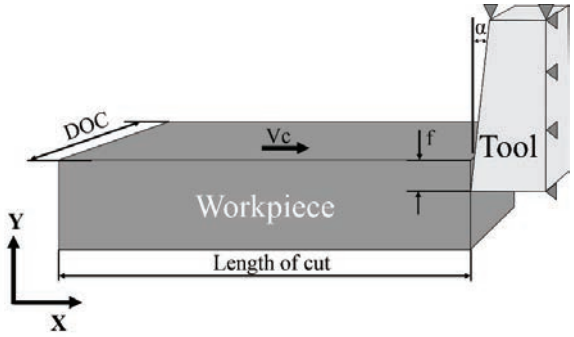

Figure 2 Schematic illustration of FE model for chip formation simulation using Thirdwave Advantedge

conductivity and specific heat. In this work, AISI 1045 steel is modeled using the power law model incorporating the influence of strain, strain rate, and temperature and is shown in Eq. (4).

$$\sigma(\varepsilon^p, \dot{\varepsilon}, T) = g(\varepsilon^p) \times \Gamma(\dot{\varepsilon}) \times \Theta(T) \quad (4)$$

with

$$(\varepsilon^p) = \sigma_0 \left(1 + \frac{\varepsilon^p}{\varepsilon_0^p}\right)^{1/n}, if\ \varepsilon^p < \varepsilon_{cut}^p$$

$$\Theta(T) = C_0 + C_1 T^1 + C_2 T^2 + C_3 T^3 + C_4 T^4 + C_5 T^5, if\ T < T_{cut}$$

$$\Theta(T) = \Theta(T_{cut}) \left(1 - \frac{T - T_{cut}}{T_m - T_{cut}}\right), if\ T > T_{cut}$$

The strain hardening component of the workpiece material model is modeled by the fitting of stress-strain curve obtained from material testing. The strain rate components are obtained from Vahid Kalhori [16]. Childs et al. [17] have shown that for all carbon steels up to 0.55%C thermal softening can be modeled in Advantedge with the parameters, C_0=1.0159, C_1=-6.8E-4 and C2-C5 = 0 with the cut-off temperature of 625 °C. The variation of thermal conductivity and specific heat capacity with temperature for AISI 1045 steel is obtained from Nandan et al. [18].

The damage model component of material modeling in Thirdwave Advantedge is defined with a damage function, D defined as

$$D = \sum_i \frac{\Delta \varepsilon_i^p}{\varepsilon_{f_i}^p} \quad (5)$$

with strain at failure ε_f^p defined as a function of temperature as shown below.

$$\varepsilon_{f0}^p = d_0 + d_1 T^1 + d_2 T^2 + d_3 T^3 + d_4 T^4 + d_5 T^5 \quad (6)$$

In this work, the damage model according to Autenrieth et al. (Figure 3) which is a function of temperature and stress triaxiality as shown in Eqn. 3 is used. The software has the capability to model the damage function only as a function of temperature as shown in Eq. (6) using a polynomial function.

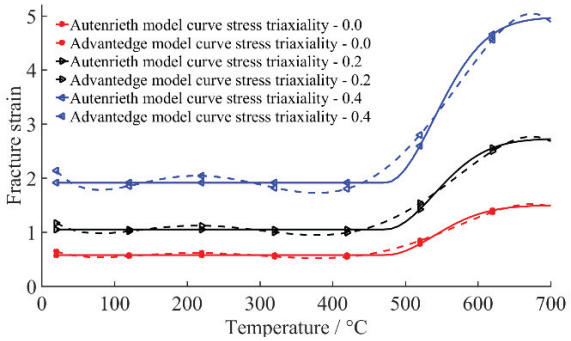

Figure 3 Variation of strain to failure with temperature and stress triaxiality

To model the Autenrieth et al.'s model in Thirdwave Advantedge, the strain to failure curves for each stress triaxiality value is modeled separately for corresponding α as shown in Table 2. The stress triaxiality values are correlated to α by considering the influence of α on the stress state in the primary deformation zone.

Table 2 Stress triaxiality factor and corresponding rake angles used in simulation.

η	0.0	0.2	0.4	0.6
α	-5°	0°	10°	20°

The friction model available with the modeling software is Coulomb friction model and the Coulomb friction factor of 1 is chosen. This represents a constant value for friction stress and is equal to $\sigma/3$ where σ represents the normal stress. The choice of this friction value is suggested for steel machining with carbide cutting tools by Childs [9]. A better approach to model friction would be to model the Coulomb friction model as a function of cutting process parameters. This approach would be taken up in the upcoming work by the authors.

4. Results

The chips obtained from the experimental investigation is presented in Figure 4 for varying f and α. The results show that with a negative α, the chips produced by all feed rates are segmented. When α is negative, i.e. -5° and f is a minimum at 0.05 mm/rev, chips with a low segmentation ratio is produced. At the same cutting conditions at a maximum f of 0.60 mm/rev, chips with high segmentation ratio are produced. When the α is +5°, the chips produced at a low f of 0.05 mm/ rev and 0.010 mm/rev were continuous, and for feed rates from 0.015 mm/rev to 0.60 mm/rev, the chips are segmented. When α was highly positive, i.e. 10° and 20°, the chips produced were continuous for all feed rates.

Figure 5. shows the simulation results for varying cutting conditions used in the experimental investigation. The

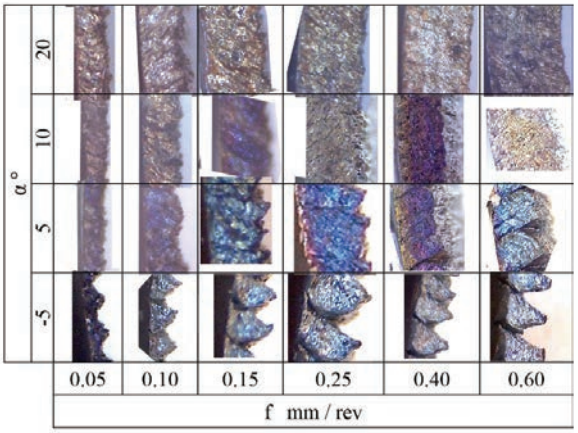

Figure 4 Chip morphology obtained from experimental investigation in machining of AISI 1045 steel for varying feed rates and rake angles.

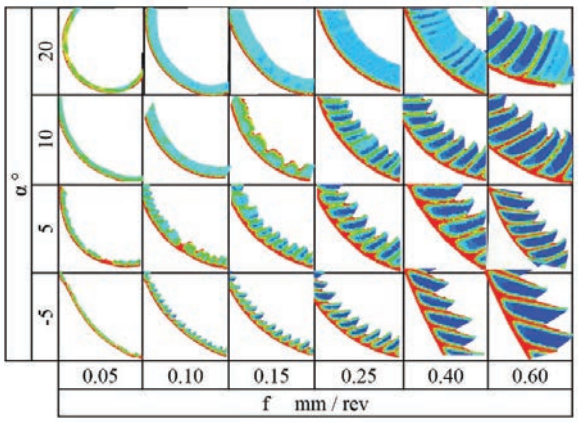

Figure 5 Chip morphology obtained from FE simulation of machining in AISI 1045 steel for varying feed rates and rake angles.

simulations predict the chips to be segmented for feed rates from 0.01 mm / rev to 0.60 mm/ rev for a α of -5°. When the αis 5°, continuous chips are predicted at lower feed rates up to 0.010 mm/rev and segmented chips for higher feed rates. The results also show that for a constant f of 0.15 mm/rev, when the α is changed from -5° to 20° the chip predicted is transformed from a segmented chip form to continuous chip. The chip segmentation frequency is measured for feed rates from 0.10 mm / rev to 0.60 mm / rev at a constant α of -5° and is plotted in Figure 5. The results from the experimental investigation show that the chip segmentation frequency reduces with the increase in f for a constant α. Figure 6 indicates that the FE model captures the trend. The results also show that chip segmentation frequency prediction error is maximum at the lowest f of 0.05 mm/rev and reduces with increasing f. The lowest chip segmentation frequency prediction error at a f of 0.60 mm/rev is still very high at 50 %.

To observe the material flow pattern in the chip under the cutting conditions where continuous chips and segmented chips are produced, the chips are observed through SEM and a representative image is shown in Figure 7. where f= 0.05 mm/rev.

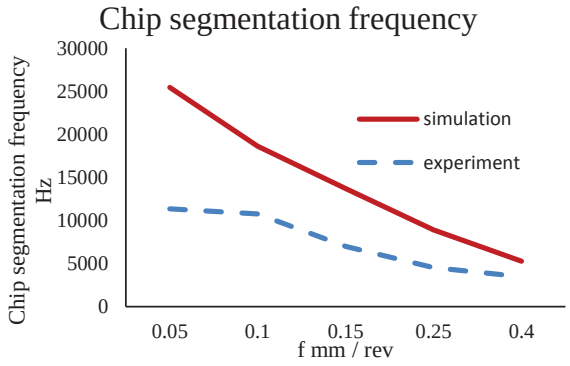

Figure 6 Chip segmentation frequency with varying f machined with α = -5°

Figure 7 shows the chip cross-section along the chip length for a negative α (top) and highly positive α (bottom). The chips obtained at the lowest feed rate-highest α cutting condition show workpiece deformation in the primary shear zone is homogeneous leading to a continuous chip. The uniform workpiece deformation is observed by a uniform deformation of the grain in the bulk area of the chip. The shear angle measured from the grain orientation in the chip has been constant along the chip length. When α=-5° segmented chips are produced and the grain orientation varies along the chip length direction clearly showing that the deformation is not homogeneous. The SEM study also shows a clear demarcation between bulk deformation in the primary shear zone and the high level of deformation in secondary shear zone leading to extremely fine grains in the range of nanometers

5. Discussion

The results from the experimental investigation show the influence of α on the transition from continuous to segmented chips at a constant vc. With a negative α, the deformation in the primary deformation zone is higher leading to a larger plastic strain in the workpiece material for all feed rates. This larger plastic strain is not homogeneous as clearly seen from the SEM analysis (Figure 7). The plastic strain is large at the shear bands (minimum chip thickness zone) and small at the bulk material (maximum chip thickness zone). The FE simulation results show that the observed chip segmentation phenomena are modeled using the strain to fracture criterion incorporating the stress triaxiality factor in the FE model employed. When the simulations were performed with the strain to fracture being modeled only as a function of temperature, the observed chip segmentation phenomena were not captured. The simulation results presented in this study show that the incorporation of the stress triaxiality factor provides the ability to predict the chip segmentation variation due to α. The simulation results also show that correlation of the rake angle with the stress triaxiality factor shown in Table 2 can predict accurately the variation of stress condition in the primary deformation zone. The simulation results show that when α is negative, a combined compression and shear loading is present in the primary deformation zone. Similarly, the simulation results also show that when α is positive (e.g. α=20°) shear loading conditions exist in the primary deformation zone.

The limitation of the software's capability to provide the damage model only as a function of temperature in the form of polynomial function leads to one constant value of stress triaxiality for each α. Due to this limitation, the variation of stress triaxiality across the primary deformation zone from the free end of the chip to the tool edge is not captured with the necessary accuracy. Future work is being planned where the work piece material model is modified according to the strain at fracture surface from Autenrieth et al [13]. This should provide the capability to predict the rake angle's influence in the primary deformation zone in its entirety.

The FE model predicts the variation of the chip segmentation frequency with increasing f. The FE model predicts a chip segmentation frequency of 25500 Hz whereas the experimental results show a chip segmentation frequency

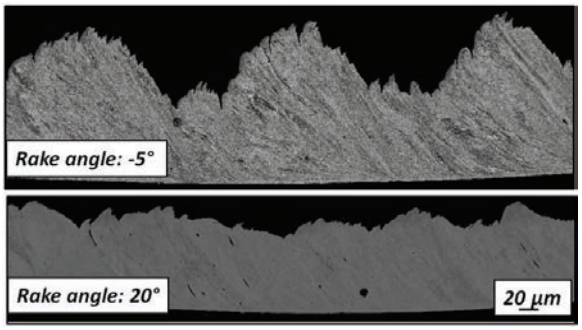

Figure 7 SEM analysis of chip at α = -5° (top) and α =20° (bottom).

of 11300 Hz. This shows that the chip segmentation phenomena are not dependent only on the deformation mechanism in the primary deformation zone but also by the deformation in the secondary deformation zone. The constant Coulomb friction model values employed in this study is a limitation and is attributed as the reason for the large quantitative error in the chip segmentation frequency prediction. The possibility to implement improved friction models as a function of the cutting process parameters is to be explored in this work.

6. Conclusion

In this study, an attempt has been made to model the variation of chip segmentation with varying α and varying f. The strain to fracture defined as a function of stress triaxiality and temperature is used to model chip segmentation in the used FE model. The study shows that the incorporation of stress triaxiality factor is necessary to capture the influence of α in the chip segmentation in the FE modeling of the cutting process. The study also shows that to improve the prediction of chip segmentation the strain to fracture model must incorporate both negative and positive values of stress triaxiality.

Acknowledgements

The authors kindly acknowledge the financial support from Sandvik Coromant and the Knowledge Foundation through the Industrial Research School SiCoMaP, Dnr 20110263, 20140130.

References

[1] K.. Nakayama, The formation of saw tooth chips, in: Proc. Int. Conf. Prod. Eng., 1974: pp. 572–577.

[2] R. Komanduri, T. Schroeder, J. Hazra, B.F. von Turkovich, D.G. Flom, On the Catastrophic Shear Instability in High-Speed Machining of an AISI 4340 Steel, J. Eng. Ind. 104 (1982) 121–131.

[3] B. Wang, Z. Liu, Serrated chip formation mechanism based on mixed mode of ductile fracture and adiabatic shear, Proc. Inst. Mech. Eng. Part B J. Eng. Manuf. 228 (2014) 181–190.

[4] C. Duan, M. Wang, A review of microstructural evolution in the adiabatic shear bands induced by high speed machining, Acta Metall. Sin. (English Lett. 26 (2013) 97–112.

[5] Z.B. Hou, R. Komanduri, Modeling of thermomechanical shear instability in machining, Int. J. Mech. Sci. 39 (1997) 1273–1314.

[6] S. Atlati, B. Haddag, M. Nouari, M. Zenasni, Thermomechanical modelling of the tool-workmaterial interface in machining and its implementation using the ABAQUS VUINTER subroutine, Int. J. Mech. Sci. 87 (2014) 102–117.

[7] S. Kouadri, K. Necib, S. Atlati, B. Haddag, M. Nouari, Quantification of the chip segmentation in metal machining: Application to machining the aeronautical aluminium alloy AA2024-T351 with cemented carbide tools WC-Co, Int. J. Mach. Tools Manuf. 64 (2013) 102–113.

[8] M. Calamaz, D. Coupard, F. Girot, A new material model for 2D numerical simulation of serrated chip formation when machining titanium alloy Ti-6Al-4V, Int. J. Mach. Tools Manuf. 48 (2008) 275–288.

[9] T.H.C. Childs, Ductile shear failure damage modelling and predicting built-up edge in steel machining, J. Mater. Process. Technol. 213 (2013) 1954–1969.

[10] G.R. Johnson, W. a Cook, Fracture characteristic of three metals subjected to various strains, strain rates, temperatures and pressures, Eng. Fract. Mech. 21 (1985) 31–48.

[11] J.R. Rice, D.M. Tracey, On the ductile enlargement of voids in triaxial stress fields, J. Mech. Phys. Solids. 17 (1969) 201–217.

[12] Y. Bai, Effect of Loading History on Necking and Fracture, 2008.

[13] H. Autenrieth, V. Schulze, N. Herzig, L.W. Meyer, Ductile failure model for the description of AISI 1045 behavior under different loading conditions, Mech. Time-Dependent Mater. 13 (2009) 215–231.

[14] C. Duan, L. Zhang, A reliable method for predicting serrated chip formation in high-speed cutting: Analysis and experimental verification, Int. J. Adv. Manuf. Technol. 64 (2013) 1587–1597.

[15] T. Marusich, M. Ortiz, Modelling and simulation of high-speed machining, Int. J. Numer. Methods Eng. 38 (1995) 3675–3694. http://onlinelibrary.wiley.com/doi/10.1002/nme.1620382108/abstract (accessed November 21, 2013).

[16] V. Kalhori, Modelling and Simulation of Metal Cutting, Luleå University of Technology, 2001.

[17] T.H.C. Childs, R. Rahmad, Modelling orthogonal machining of carbon steels. Part II: Comparisons with experiments, Int. J. Mech. Sci. 51 (2009) 465–472.

[18] R. Nandan, G.G. Roy, T.J. Lienert, T. Debroy, Three-dimensional heat and material flow during friction stir welding of mild steel, Acta Mater. 55 (2007) 883–895.